# Temperature-dependent photon scattering in blue-detuned optical traps

Matthew L. Terraciano, Spencer E. Olson, and Fredrik K. Fatemi
*Naval Research Laboratory, 4555 Overlook Avenue S.W., Washington, D.C. 20375, USA*
(Received 18 May 2011; published 3 August 2011)

We have observed time-varying spin relaxation of trapped cold atoms due to photon scattering in blue-detuned, crossed, hollow Laguerre-Gaussian beams. These beams are formed by imparting an azimuthal phase of $\ell\phi$ to a Gaussian beam, where $\ell$ is an integer, and have an intensity distribution that scales with $r^{2\ell}$ to the lowest order. For all degrees of anharmonicity, we observe a time-varying spin-relaxation rate due to energy-dependent photon scattering. For $\ell = 8$, we directly measure temperature-dependent scattering rates and show that by removing the most energetic atoms from the trap, a more purely spin-polarized sample remains. The results agree well with Monte Carlo simulations, and we present a simple functional form for the spin-relaxation curves.

DOI: 10.1103/PhysRevA.84.025402 PACS number(s): 37.10.Gh, 37.10.Vz

The optical dipole force on an atom exposed to an off-resonant, spatially varying light field depends on the sign of the detuning [1]. When a laser field is tuned above (below) the atomic resonance, the force is repulsive (attractive). Optical traps are useful for atom storage and guiding, and for precision measurements when magnetic traps cannot be used or when all spin states must be trapped (e.g., spinor condensates [2–4]). Such traps also extend quantum memory, which can benefit from magnetic field suppression [5]. For red-detuned traps, large detunings are required for negligible photon scattering [6], but they are impractical for large volume atom trapping.

In contrast, a blue-detuned optical trap can be simultaneously deep and large volume, with relatively low laser power, and by keeping the atoms in the dark, can exhibit low photon-scattering rates [7–10]. Because the light only defines the trap boundaries, traps can be made over a wide variety of surface-to-volume ratios and profiles, or optimized for darkness, large atom-number confinement, etc. We recently used these properties of dark traps for magnetometry with high duty cycle [7,11] in crossed, high-charge-number, hollow laser beams. Furthermore, the controllable anharmonicity of these beams makes them ideal for studying Bose-Einstein condensation (BEC) vortex formation [12,13], and recently they have been investigated for fundamental studies of BEC in power-law traps [14,15]. Because blue-detuned traps are often operated near resonance, scattering can no longer be neglected. Thus, an understanding of scattering in dark traps near resonance is required for optimal use of available laser parameters. Scattering rates have been measured in some limited trap types [8–10], but to the best of our knowledge, experimental comparisons between trap types under similar conditions have not been done.

In this Brief Report, we measure the spontaneous Raman scattering rate from $^{87}$Rb atoms confined to traps with different degrees of anharmonicity. Although it is not surprising that boxlike intensity distributions are favored for reduced photon scattering over harmonic profiles, the results reported here expose common behaviors among all blue-detuned traps. We experimentally observe a time-varying spin-relaxation rate in blue-detuned traps due to the dependence of the photon-scattering rate on the atom energy. We demonstrate the effect of ensemble temperature on the depolarization, and further observe the energy-dependent rates within the ensemble. The results agree well with Monte Carlo simulations.

Figure 1 shows the optical layout of the experiment. Our hollow beam trap is relayed to intersect itself at right angles by an $8f$ imaging relay, as described in Ref. [16]. The hollow beams are formed by modifying the wave front phase of a Gaussian beam with a reflective spatial light modulator (SLM, Boulder Nonlinear Systems), which allows trapping geometries to be compared without other changes. SLMs are valuable in cold-atom experiments because of their ability to control trap parameters in a programmable manner [16–19]. The applied phase has a profile $\Psi(\rho,\phi) = \ell\phi + f\lambda/\pi\rho^2$, where $\rho$ and $\phi$ are cylindrical coordinates, $\ell$ is an integer, and $\lambda$ is the wavelength. The charge number $\ell$ controls the anharmonicity and produces an intensity profile that scales with $\rho^{2\ell}$ to the lowest order. The second term is a controllable lens function of focal length $f \approx 200$ mm to focus the beam onto the atom sample. Modifying a Gaussian beam with $\Psi(\rho,\phi)$ results in a close approximation to the Laguerre-Gaussian $\mathrm{LG}^{\ell}_{p=0}$ mode, where $p$ and $\ell$ are the radial and azimuthal indices [20]. For $\ell \geqslant 4$, we operate the trap a few centimeters away from the focal plane, where aberrations are reduced and the peak intensity is maximum [20].

The light for the hollow beam is derived from a tunable, extended-cavity diode laser, amplified to 1200 mW by a tapered amplifier. The total power delivered to the experiment is controlled by an acousto-optic modulator (AOM). We couple up to 350 mW into the polarization-maintaining (PM) optical fiber. Residual resonant light from amplified spontaneous emission is filtered out by a heated vapor cell. The fiber output is collimated to a $1/e^2$ waist of 1.71 mm, and modified by the SLM, which has ≈80% diffraction efficiency. Images and profiles of the beams at the trap location are shown in Fig. 1, and these beams provide a useful way to readily compare traps of polynomial degree $2\ell$. In this Brief Report, we use the variation of the anharmonicity to demonstrate the general effect of time-varying spin-relaxation rates in blue-detuned traps.

Our experiment begins with cold $^{87}$Rb atoms derived from a magneto-optical trap (MOT). We confine $\approx 10^7$ atoms in a ≈500-$\mu$m-diameter ($1/e^2$) cloud. The atoms are further cooled in a 10-ms-long molasses stage to ≈10 $\mu$K, after which all MOT-related beams are extinguished. The 440-$\mu$m-diameter

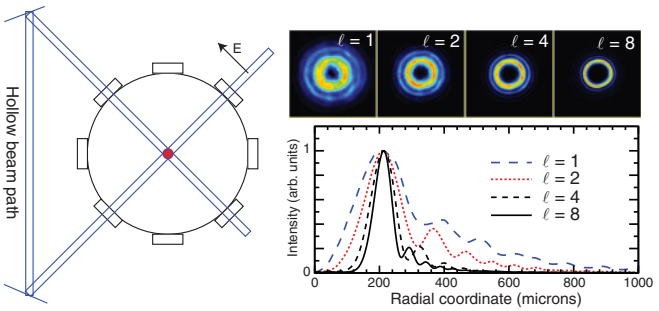


FIG. 1. (Color online) Left: Layout of the trapping beams. Lenses used in the bowtie relay are not shown. Polarization is in the figure plane to reduce interference effects. Right: Cross-sectional intensity distributions for hollow beams with charge numbers $\ell$ = 1, 2, 4, and 8.

hollow beam trap is on throughout the MOT loading. We observe no dependence on how the hollow beam trap is turned on. We use all available power regardless of $\ell$, so the peak intensity is $\ell$ dependent. For $\ell = 2$, 4, and 8, we get $I_{\max} =$ 79, 125, and 290 W/cm$^2$, respectively.

We measure the relaxation of hyperfine populations after optically pumping all atoms to the lower ($F = 1$) hyperfine level [8]. Following the molasses stage, the atoms are trapped only by the hollow beams and are pumped into the $F = 1$ hyperfine level after atoms outside the trap volume have fallen away (≈50 ms). After a variable trapping time $T$, the trap light is extinguished and the atoms are exposed to a 50 $\mu$s pulse on the cycling transition connecting $F = 2 - F' = 3$ to measure the excited atom number, followed by a 100 $\mu$s pulse containing both repump and cycling light for normalization. Fluorescence from the pulses is detected by a photomultiplier. The ratio of the relative atom numbers is the excited hyperfine fraction $N(t)$, which approaches $C = 5/8$ for $^{87}$Rb.

Figure 2(a) shows the spin-relaxation curves for $\ell = 2$, 4, and 8 for a detuning $\Delta = 0.25$ nm. Instead of plotting $N(t)$, we plot $C - N(t)$ on a logarithmic scale to highlight the deviation of the polarization decay from a pure exponential. Clearly, the higher-charge-number traps lead to a longer spin-relaxation time, despite having a higher peak intensity, highlighting the benefit of increased $\ell$. We made similar measurements with constant peak intensity but the results are qualitatively the same.

The main motivation for this work, however, is the clear nonlinearity of the relaxation curves in Fig. 2(a), first observed in Ref. [8], indicating a gradual slowing of the spin-relaxation rate. Fits to the excited fraction using

$$N(t) = C[1 - \exp(-t/\tau)] \tag{1}$$

(shown explicitly for $\ell = 2$) underestimate $N(t)$ at early times and overestimate it at long times. We find $\tau = 89$, 147, and 225 ms, respectively, for $\ell = 2$, 4, and 8. To accommodate this change, we also show, in Fig. 2(a), fits with time-varying $\tau(t) = \tau_0[1 + (t/\tau_1)^{0.5}]$, to be discussed later, where $\tau_0$ is the initial relaxation time and $\tau_1$ is the doubling time. The respective fit parameters are $\tau_0 = 27$, 73, and 101 ms; and $\tau_1 = 17$, 145, and 140 ms for $\ell = 2$, 4, and 8, respectively. This rate-changing spin relaxation also occurs for larger detuning; in Fig. 2(b), we show the curve for $\ell = 8$ at $\Delta = 1.0$ nm

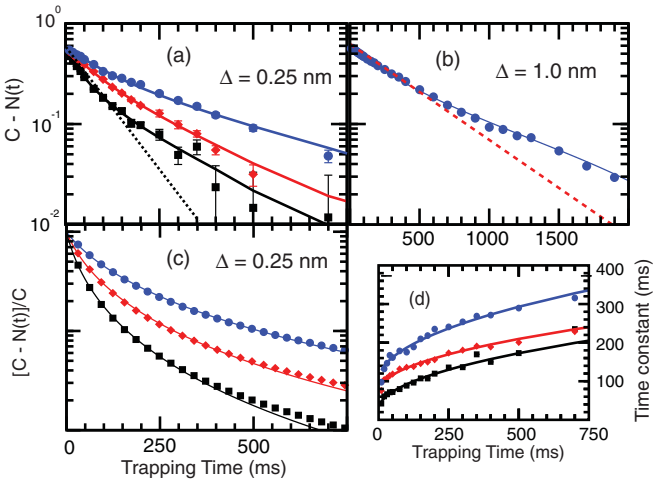


FIG. 2. (Color online) (a) Spin-polarization curves for different $\ell$. $\ell = 2$ (black squares), $\ell = 4$ (red diamonds), and $\ell = 8$ (blue circles) with fits to Eq. (1). Deviation from linearity is shown for $\ell = 2$ (dotted line). (b) Curve for $\Delta = 1.0$ nm with exponential fit (dotted line) and chirped exponential fit (solid). (c) Curves using a simple three-level treatment [same legend as (a)]. (d) Instantaneous time constant for $\ell = 2$, 4, and 8 [same legend as (a)].

($\tau_0 = 275$ ms, $\tau_1 = 1055$ ms). The time variation of $\tau(t)$ is explicitly plotted in Fig. 2(d), by solving for it in Eq. (1). We observed this general behavior for all blue-detuned trap types near resonance, including the harmonic toroidal trap in Ref. [8].

This chirped relaxation rate is due to the distribution of energies within the trapped ensemble. The spin-relaxation rate is proportional to the intensity that the atom samples. Higher intensities are sampled by the more energetic atoms, so any thermal distribution of atoms will result in a distribution of relaxation rates, provided the rethermalization rate is lower than the relaxation rate. Furthermore, we point out that when the photon-scattering rate becomes long compared to the rethermalization rate, the depolarization within the ensemble is isotropic, and we expect to recover a constant relaxation rate. Thus, the ratio $\tau_0/\tau_1$ should approach 0 for large detuning. We observe this general trend in our results. For the fastest relaxation curve ($\Delta = 0.25$ nm, $\ell = 2$), the ratio $\tau_0/\tau_1$ is 1.6. For $\Delta = 1$ nm, $\ell = 8$, the ratio has reduced to 0.26.

Previous analytical treatments predict a temperature-dependent ensemble heating rate [1], which we will show experimentally in this work though spin-relaxation measurements. To expose the main features of the relaxation curves, we briefly examine relaxation in a three-level atom.

For a three-level atom, the excited fraction is

$$N(t) = C\{1 - \exp[-(\gamma_{12} + \gamma_{21})t]\}, \tag{2}$$

where $C = \gamma_{12}/(\gamma_{12} + \gamma_{21})$, and $\gamma_{12}$ and $\gamma_{21}$ are the scattering rates for transitions to and from the $F = 2$ hyperfine level ($C = 5/8$ for $^{87}$Rb). In this simple treatment, we neglect gravity. For detunings much smaller than the fine-structure splitting, $\gamma_{12}$ and $\gamma_{21}$ are similar in magnitude to the recoil photon scattering rate $\gamma$:

$$\gamma_{12} + \gamma_{21} \propto \gamma = \langle U(I) \rangle \frac{\Gamma}{\Delta}. \tag{3}$$

By the virial theorem, for a potential $U \propto \rho^{2\ell}$, $\langle U \rangle = E/(1+\ell)$, and $E$ is the total energy. Thus, we have

$$\gamma = \frac{\Gamma}{\Delta}\frac{E}{1+\ell}, \tag{4}$$

where $E = a_\ell \rho_0^{2\ell} + 0.5 M v_0^2$; $\rho_0$ and $v_0$ are the starting position and speed; and $M$ is the atom mass. The time-averaged intensity to which the atom is exposed is reduced by $1/(1+\ell)$, while the time-varying scattering rate derives from the dependence on $E$.

To find the total number of excited atoms, we integrate over all starting positions and velocities in the trap volume. We use the experimental values of $T = 10\ \mu$K, $\Delta = 0.25$ nm, and choose $a_\ell$ for equal trap depth at the beam radius. Curves for purely anharmonic potentials are shown in Fig. 2(c), showing the nonlinear rate. To account for this nonlinearity, $\tau$ in Eq. (1) is written as

$$\tau(t) = \tau_0[1 + (t/\tau_1)^c], \tag{5}$$

where $\tau_0$ is the time constant at $t = 0$, and $\tau_1$ is the doubling time. Although $c$ could also be left as a fit parameter, we typically find that the best values are obtained for $0.5 \leqslant c \leqslant 0.8$. We stress that $\tau_1$ and $c$ are phenomenological constants introduced to provide an intuitive picture for the rate change compared with the single-parameter exponential typically used in scattering measurements [10,21]. Additional parameters will always improve the fit, but this form presents a simple physical picture and allows estimation of the relaxation rate at various trap times.

We note that while this simple treatment demonstrates the key points (nonlinearity due to thermal spread and the effect of $\ell$), and can be used to predict the qualitative effects of various trap parameters, it generally overestimates the relaxation rate. This is because it uses a purely anharmonic potential ($U \propto \rho^{2n}$), which, unlike the actual potential, continues to increase. However, it does provide a rough approximation of the relaxation rates. Indeed, this treatment gives $\tau_0 = 26$, 43, and 79 ms, whereas the experiment gave 27, 73, and 101 ms. Below, we use Monte Carlo simulations employing the experimental trap characteristics, gravity, and spontaneous Raman scattering formulas to accurately model the behavior [8,21].

Virial theorem arguments have also been used in Ref. [1] to predict an overall temperature-dependent heating rate of the ensemble. Below, we experimentally demonstrate temperature-dependent spin relaxation, and further observe the energy dependence of relaxation within the ensemble.

To measure spin relaxation at different temperatures, we adjust the average energy of the trapped cloud, as shown in Fig. 3(a) (inset). The atoms are first trapped in the crossed beam with $\ell = 8$ and $\Delta = 0.25$ nm. We force more energetic atoms to leave the trap by lowering the laser power to $P_{\min}$ over 30 ms, then increasing it back to the original power $P_0$ over 30 ms. We do this for four different values of $P_{\min}$ from 0.1–1.0$P_0$. Figure 3(a) shows that as $P_{\min}$ is decreased and more energetic atoms are released, the relaxation rate also decreases. When $P_{\min}$ is $0.1P_0$, $\tau_0$ increases from ≈100 to ≈170 ms.

We have studied this in more detail by running simulations of the relaxation rate for initial atom temperatures between

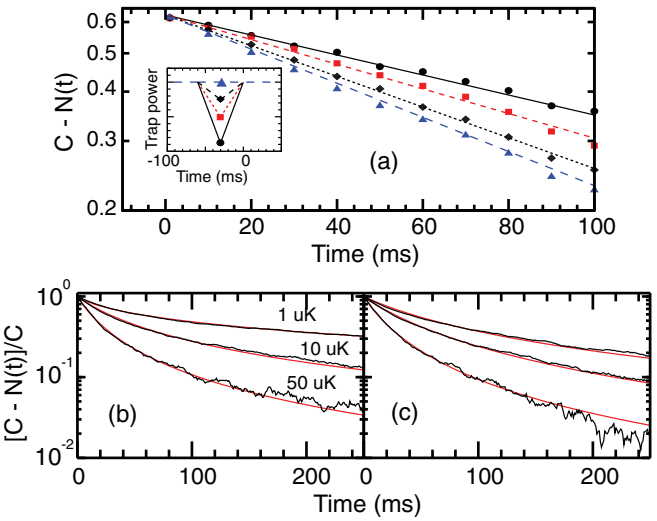


FIG. 3. (Color online) (a) Scattering curves at early times for the temporal intensity profiles shown in the inset. (b) Simulations of polarization as a function of time without gravity, and (c) with gravity. Gravity reduces relaxation times as the atoms are supported by the light field.

1–50 $\mu$K, as described in Ref. [8]. The temperature dependence is shown in Figs. 3(b) and 3(c). We fit these simulations to Eq. (5) using $c = 0.8$. The effect of gravity is to reduce the overall scattering time, since the optical trap provides the support against gravity. For our trap size with $R = 220\ \mu$m, the gravitational potential energy is $U_g \approx 30\ \mu$K. When the atom energy distribution is well below this, gravity has a large effect. As the atom energy increases, the relative effect of gravity is reduced and the scattering times are similar.

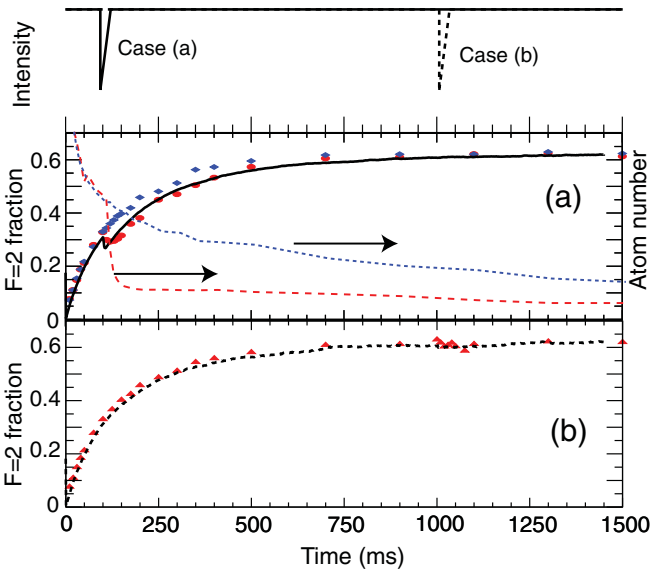


FIG. 4. (Color online) Scattering curves after releasing higher-energy-trapped atoms; the temporal intensity profiles are shown at top. Drop time = (a) 100 and (b) 1000 ms. In (a) we show the curve for the constant intensity profile (blue diamonds) and ramped intensity profile (red circles). Atom numbers are shown for the constant intensity (blue dotted line) and for the ramped intensity (red dashed line). Errors are within the symbol size.

Specifically, though, we find similar values for $\tau_0$ with and without gravity (72, 40, and 18 ms for $T = 1$, 10, and 50 $\mu$K, respectively), and the values of $\tau_1$ are different, particularly for colder samples: With gravity, we find $\tau_1 = 110$, 100, and 61 ms; without gravity, $\tau_1 = 280$, 160, and 72 ms for $T = 1$, 10, and 50 $\mu$K, respectively.

The fact that the higher energy atoms scatter photons more quickly means that the lower energy atoms within the ensemble have a higher degree of spin polarization. While the preceding results showed that a hotter sample depolarizes more quickly, here we show that removal of the higher energy atoms within the sample leads to increased spin polarization. To show this, we first hold the atoms for 100 ms, then lower the laser power to remove the hotter atoms, and ramp it back up linearly over 30 ms [Fig. 4(a)]. If spin depolarization were isotropic, there would be no effect on the excited fraction, but some of the depolarization is carried away by the removal of the energetic atoms. The total atom number dropped by a factor of three during this process. We did the same measurement after $T = 1$ sec [Fig. 4(b)], when the sample was completely depolarized. At this point, there is no spin anisotropy and no effect on the excited fraction. Our results also neglect other effects of rethermalization such as hyperfine changing collisions, which could drastically change the degree of spin polarization. At our densities of $10^{10}$ atoms/cm$^3$, this effect is negligible, but spin relaxation in higher density samples could be an interesting area to explore.

In conclusion, we have experimentally observed time-dependent spin relaxation for atoms confined to dark optical traps with different power laws. The behavior was seen regardless of trap anharmonicity, due to the energy distribution in the trap. The results agreed well with Monte Carlo simulations.

This work was funded by the Office of Naval Research.

[1] R. Grimm, M. Weidemuller, and Y. B. Ovchinnikov, Adv. At. Mol. Opt. Phys. **42**, 95 (2000).
[2] A. T. Black, E. Gomez, L. D. Turner, S. Jung, and P. D. Lett, Phys. Rev. Lett. **99**, 070403 (2007).
[3] M. Vengalattore, J. M. Higbie, S. R. Leslie, J. Guzman, L. E. Sadler, and D. M. Stamper-Kurn, Phys. Rev. Lett. **98**, 200801 (2007).
[4] J. Stenger, S. Inouye, D. M. Stamper-Kurn, H. J. Miesner, A. P. Chikkatur, and W. Ketterle, Nature (London) **396**, 345 (1998).
[5] C.-S. Chuu, T. Strassel, B. Zhao, M. Koch, Y.-A. Chen, S. Chen, Z.-S. Yuan, J. Schmiedmayer, and J.-W. Pan, Phys. Rev. Lett. **101**, 120501 (2008).
[6] N. Davidson, H. J. Lee, C. S. Adams, M. Kasevich, and S. Chu, Phys. Rev. Lett. **74**, 1311 (1995).
[7] M. L. Terraciano, M. Bashkansky, and F. K. Fatemi, Phys. Rev. A **77**, 063417 (2008).
[8] S. E. Olson, M. L. Terraciano, M. Bashkansky, and F. K. Fatemi, Phys. Rev. A **76**, 061404 (2007).
[9] A. Kaplan, M. F. Anderson, T. Grunzweig, and N. Davidson, J. Opt. B **7**, R103 (2005).
[10] N. Friedman, A. Kaplan, and N. Davidson, Adv. At. Mol. Opt. Phys. **48**, 99 (2002).
[11] F. K. Fatemi and M. Bashkansky, Opt. Express **18**, 2190 (2010).
[12] V. Bretin, S. Stock, Y. Seurin, and J. Dalibard, Phys. Rev. Lett. **92**, 050403 (2004).
[13] G. M. Kavoulakis and G. Baym, New J. Phys. **5**, 51 (2003).
[14] A. Jaouadi, M. Telmini, and E. Charron, Phys. Rev. A **83**, 023616 (2011).
[15] A. Jaouadi, N. Gaaloul, B. Viaris de Lesegno, M. Telmini, L. Pruvost, and E. Charron, Phys. Rev. A **82**, 023613 (2010).
[16] F. K. Fatemi, M. Bashkansky, and Z. Dutton, Opt. Express **15**, 3589 (2007).
[17] N. Chattrapiban, E. A. Rogers, I. V. Arakelyan, R. Roy, and W. T. H. III, J. Opt. Soc. Am. B **23**, 94 (2006).
[18] S. Bergamini, B. Darquié, M. Jones, L. Jacubowiez, A. Browaeys, and P. Grangier, J. Opt. Soc. Am. B **21**, 1889 (2004).
[19] D. McGloin, G. C. Spalding, H. Melville, W. Sibbett, and K. Dholakia, Opt. Express **11**, 158 (2003).
[20] F. K. Fatemi and M. Bashkansky, Appl. Opt. **46**, 7573 (2007).
[21] R. A. Cline, J. D. Miller, M. R. Matthews, and D. J. Heinzen, Opt. Lett. **19**, 207 (1994).